Accepted Manuscript

Precipitation in a novel maraging steel F1E: A study of austenitization and aging using small angle neutron scattering

V. Gray, D. Galvin, L. Sun, E.P. Gilbert, T. Martin, P. Hill, M. Rawson, K. Perkins

PII: S1044-5803(17)30258-9
DOI: doi: 10.1016/j.matchar.2017.05.002
Reference: MTL 8663

To appear in: *Materials Characterization*

Received date: 27 January 2017
Revised date: 24 April 2017
Accepted date: 3 May 2017

Please cite this article as: V. Gray, D. Galvin, L. Sun, E.P. Gilbert, T. Martin, P. Hill, M. Rawson, K. Perkins , Precipitation in a novel maraging steel F1E: A study of austenitization and aging using small angle neutron scattering, *Materials Characterization* (2017), doi: 10.1016/j.matchar.2017.05.002

Precipitation in a novel maraging steel F1E: A study of austenitization and aging using small angle neutron scattering

V. Gray[1], D. Galvin[1], L. Sun[2], E. P. Gilbert[3], T. Martin[4], P. Hill[5], M. Rawson[5] and K. Perkins[1]

1. Institute of Structural Materials, Swansea University, Swansea SA1 8EN, UK.

2. Department of Materials Science and Metallurgy, University of Cambridge, Cambridge CB2 1TN, UK.

3. Australian Centre for Neutron Scattering, Australian Nuclear Science & Technology Organisation, Lucas Heights NSW 2234, Australia.

4. Department of Materials, University of Oxford, Parks Road, Oxford OX1 3PH, UK.

5. Rolls-Royce plc., PO Box 31, Derby DE24 8BJ, UK.

Corresponding Author: V. Gray, v.a.gray@swansea.ac.uk

Graphical Abstract

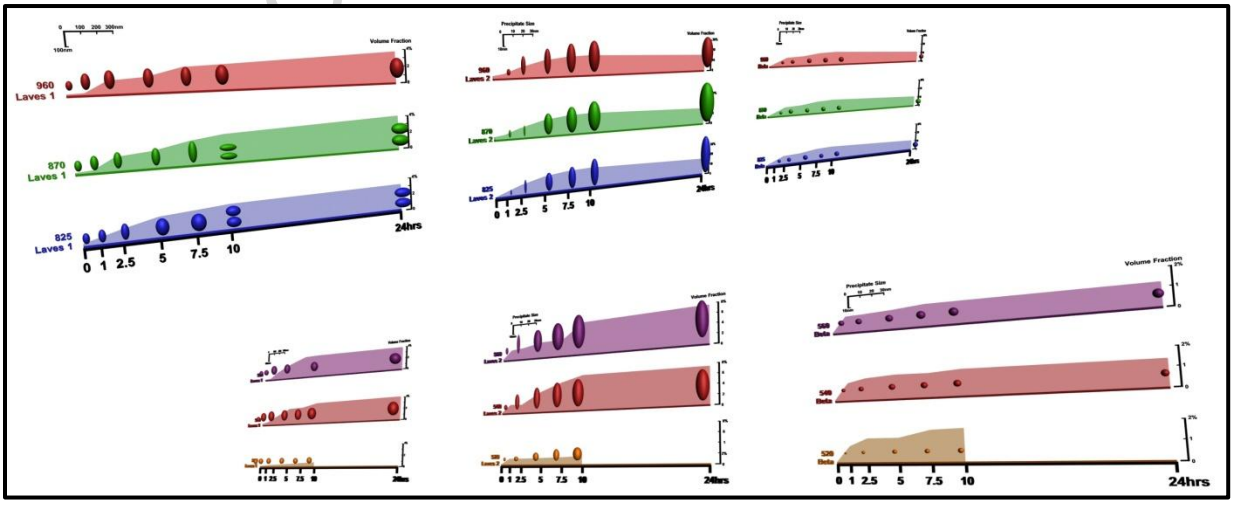

Abstract

The effect of austenitization temperature, aging temperature, and, aging time on the development of precipitates in a novel maraging steel known as F1E was investigated. The investigation primarily employed small angle neutron scattering (SANS) coupled with thermal calculations, atom probe tomography (APT) and electron microscopy (SEM, STEM, TEM). This large scale study investigated austenitization temperatures of 825, 870 and 960°C with aging of 0, 1, 2.5, 5, 7.5, 10 and 24 hrs conducted at 540°C. For austenitization at 960°C, aging at 520°C and 560°C was also conducted for the same aging times. This yielded 32 conditions where the size, shape and volume fraction of three different precipitates were determined, namely a pre-existing laves phase, a developing laves phase, and a developing β phase. Also observed in this study was a significant change in microstructure of the pre-existing laves precipitate as a result of aging time.

Keywords: SANS; steel; maraging; precipitation; aging

1. Introduction

Maraging steels are low carbon-high strength steels that derive their properties from the formation of intermetallic precipitates nucleating in the martensitic matrix during thermal ageing treatments [1]. Their enhanced properties are suited to applications such as gears and shafts, especially for the aerospace industry which continually requires materials to operate at higher stresses and temperatures with each new generation of engine [2]. Here, Small Angle Neutron Scattering (SANS) is used to study the development of precipitates over a large array of austenitization and aging conditions for a maraging steel more commonly known as F1E,

which currently shows more desirable material properties than its current competitors: AerMet 100 and Super CMV [3].

After an austenitization process, the steel is air quenched to room temperature resulting in a martensitic microstructure which is then isothermally aged to exploit precipitation strengthening effects, specifically to optimise mechanical properties such as strength, toughness and fatigue resistance through continuing and initiating precipitate growth on dislocations, as well as, at martensitic and prior-austenite grain boundaries. [4,5]. McAdams found higher austenitization temperatures reduce hardness in the unaged condition, but once aged or thermally exposed, hardness increased with higher austenitization temperature [3]. This was attributed to precipitate coarsening even though higher austenitization temperature is known to have fewer precipitates, significantly so in some cases [3]. Room temperature tensile testing of F1E austenitized at 825, 870 and 960 °C yielded ductilities of ~8%, ~4% and ~6% respectively. When the same test was conducted at 450 °C after 5 hrs aging this trend reversed with the 870 °C material recording an elongation approximately 1.5 times that of both the 825 and 960 °C austenitization conditions. It is thought these non-intuitive changes in mechanical properties stem from the evolution of the two known precipitates of F1E: (i) a tungsten-molybdenum rich laves phase [$(Fe,Cr)_2$ (Mo,W)] [3] that reportedly pins the martensite lath boundaries promoting creep resistance and microstructural stability [6], and, (ii) a nickel-aluminium rich β phase (NiAl) which provides both strength and ductility.

SANS was used to observe precipitation behaviour over a large array of austenitization and thermal aging conditions. Samples following austenitization at 825, 870 and 960 °C and thermal aging at 540 °C for 0, 1, 2.5, 5, 7.5, 10 and 24 hrs were observed to examine the effect of austenitization conditions on precipitate development. For the 960 °C

austenitization condition, thermal aging was also conducted at 520 and 560 °C for 1, 2.5, 5, 7.5, and 10 hrs to observe the effect of thermal aging temperature on precipitate development. SANS has been used in conjunction with a number of other techniques such as thermal calculations, atom probe tomography (APT), and scanning, scanning transmission and transmission electron microscopy (SEM, STEM, TEM) to examine a total of 32 different austenitization and aging treatments.

2. Samples

The material was provided by Rolls-Royce plc. [7] in as cast-bars manufactured by ATI Allvac, USA [8] with the general composition given in Table 1. It was manufactured by the VIM/VAR process before homogenisation and hot rolling thus eliminating any precipitates. Cubes measuring 20x20x20mm were then austenitized at 825, 870 or 960 °C for 1 hour in a laboratory carbolite furnace before air-quenching to room temperature. They were then individually aged at 520, 540 or 560 °C for 1, 2.5, 5, 7.5, 10 and 24 hours. Samples were cut into squares of 10x10mm with a thickness of approximately 700 μm and ground to a thickness of 300 μm using 1200-600 grit paper to obtain optimal neutron transmission. A summary of the austenitization and thermal aging conditions examined is given below in Table 2.

Table 1. Nominal composition of maraging steel F1E in %wt.

C	Cr	Mo	Ni	Al	Co	W	B	Fe
0.003	10	2.75	7	1.8	8.3	2.45	0.002	% Balance

Table 2. Summary of test conditions: austenitization temperature, aging temperature and aging time

Aging Time (hrs)	Austenitization Temperature-Aging Temperature (°C)				
0	825	870	-	960	-
1	825-540	870-540	960-520	960-540	960-560
2.5	825-540	870-540	960-520	960-540	960-560
5	825-540	870-540	960-520	960-540	960-560
7.5	825-540	870-540	960-520	960-540	960-560
10	825-540	870-540	960-520	960-540	960-560
24	825-540	870-540	-	960-540	960-560

3. Experiment

3.1 Other Techniques

Although this research focuses on the results of SANS, a number of other complementary techniques were used to build a comprehensive picture of precipitation behaviour.

Thermal Calculations

Thermal calculations were conducted using MTDATA [9] with resultant phase information shown in Fig. 1. For austenitization at 825 and 870 °C the unaged conditions are expected to contain a small amount of laves precipitation, whereas the 960 °C samples should contain no or minimal precipitates with any laves phase expected to be completely in solution with the austenite above approximately 930 °C. Aging at 520, 540 and 560 °C both laves and β phase precipitates are expected to nucleate and grow, with β precipitate growth fairly uniform noting the change in growth rate expected at 600 °C.

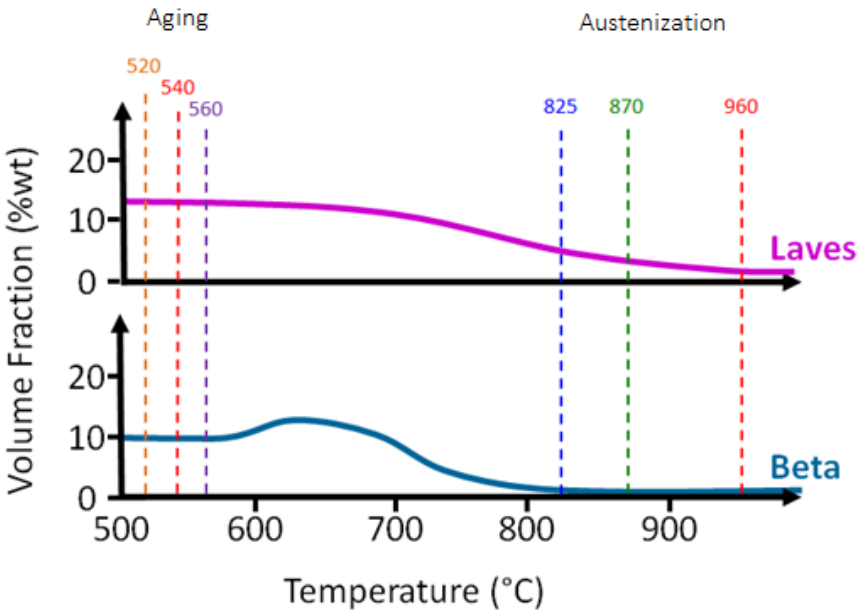

Figure 1. Thermal calculations of phases present in F1E

Atom Probe Tomography (APT)

Samples were prepared using electropolishing and focused ion beam (FIB) liftout. Matchsticks of 0.5×0.5×20 mm were electropolished using a solution of 25% perchloric acid and 75% glacial acetic acid at a DC voltage of 14 V until a neck formed allowing for separation into two needle-shaped specimens [10]. Needles were refined using a polishing solution of 2% perchloric acid in butoxyethanol.

Using APT, the composition of the matrix and precipitates were determined for the unaged and 5 hr thermally aged condition at 540 °C with a general composition given in Table 3. Knowing the unaged and 5 hr aged composition, compositions for 1 and 2.5 hrs were linearly interpolated between these known values, whilst, for aged conditions over 5 hrs the composition was held constant.

Table 3. General composition of unaged maraging steel F1E laves and β precipitates by %wt.

	C	Cr	Mo	Ni	Al	Co	W	Fe
Laves	0.02	7	24.5	1	0.2	3.6	32.9	% Balance
β	0	3.8	0.9	36.1	22.2	5.9	0.5	% Balance

Electron Microscopy (EM)

Electron microscopy provides insight into the precipitates present in F1E. Dark field TEM reveals the laves phase in Fig. 2c, and the β phase in Fig. 2d [3]. An approximate volume fraction of precipitates at the 825 °C austenitized condition aged at 540 °C for 5 hrs is ~6.5% laves and ~1.8% β phase. Using STEM, Fig. 3 shows two populations of laves with the larger present from austenitization, and the smaller nucleating during aging. Both these particles have an irregular elliptical shape in contrast to the spherical β phase shown in Fig 2d. When observed by TEM, laves from austenitization form in the laths, whilst nucleating laves form within the matrix in clusters.

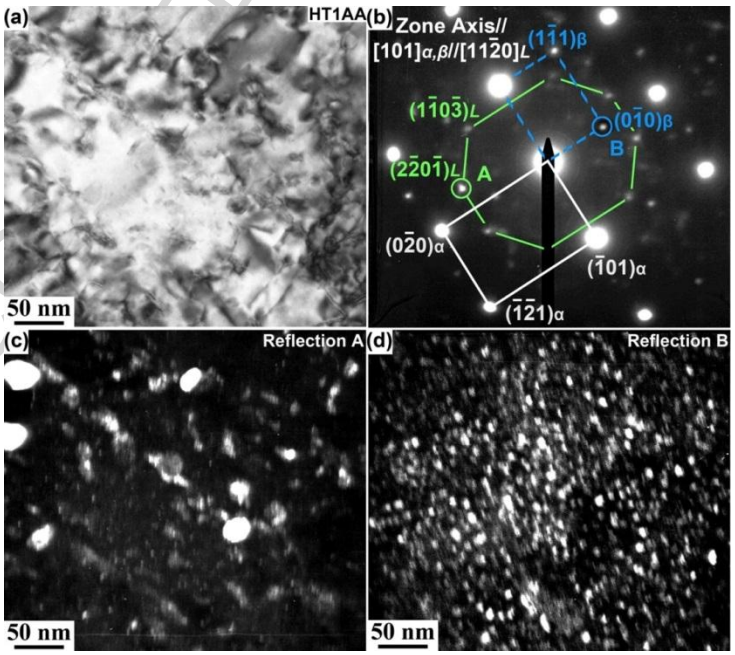

Figure 2. TEM for austenitized at 825 °C and aged at 540 °C for 5 hrs: a) bright field image, b) lattice reflections, c) dark field image of laves, and d) dark field image of β phase

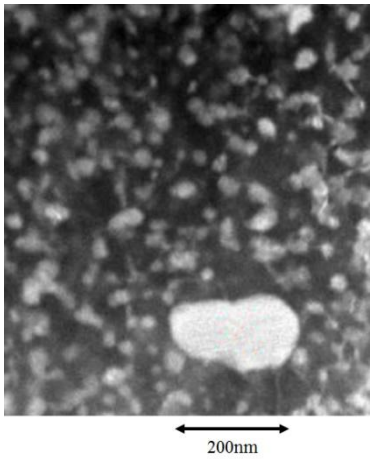

Figure 3. STEM image of F1E microstructure. Austenitized at 960°C and aged 5 hrs at 540°C. Reproduced from [3].

3.2 SANS

Small Angle Neutron Scattering (SANS) experiments were conducted on the QUOKKA instrument at the OPAL reactor at ANSTO, Australia [11]. Three configurations were used to cover a q range of ~0.003 to 0.74 $Å^{-1}$ where q is the magnitude of the scattering vector defined as $q=4\pi/\lambda.sin\theta$, where λ=5 Å with $\Delta\lambda/\lambda$=10% resolution and 2θ the scattering angle. The configurations were L_1=L_2=20 m, L_1=L_2=12 m, and L_1=12 m L_2=1.3 m, where L_1 and L_2 are source-to-sample and sample-to-detector distances, and with source and sample apertures of 50 mm and 5 mm diameter respectively. The latter yielded an illuminated average sample volume of 6 mm^3. SANS data were reduced using NCNR SANS reduction macros modified for the QUOKKA instrument, using Igor software package [12] and transformed to absolute scale by the use of an attenuated direct beam transmission measurement [13-14]. The spectra were then analysed using in-built algorithms within the SASview package [15-21].

In this experiment total scattering (nuclear and magnetic) was observed. For the precipitates, their chemistry was known from APT and approximate volume fractions and size was known

from SEM, TEM and APT for a number of conditions. Given their non-magnetic nature and the ability to corroborate size and volume fraction from other methods mentioned above, total scattering was chosen. When considering the matrix which is ferromagnetic, the scattering from it includes scattering over the magnetic domain. As the matrix also contains super laves measuring ~1 μm (not distinguishable due to the limited q range), a matrix function was chosen in order to eliminate this phase from analysis with no size or volume fraction determined from the matrix function. Using progressively fitted spectra with increasing aging time, total scattering produced results consistent with other APT, SEM, TEM, and STEM observations and thus is considered to be reliable in the interim conditions observed using only SANS.

The system under observation in this experiment has 4 different phases; (i) matrix, (ii) pre-existing laves ~120nm, (iii) nucleating laves ~30nm, and, (iv) β phase ~5nm. The unaged samples are known to contain matrix and pre-existing laves which are modelled by a Guinier-Porod and ellipsoid function. The Guinier-Porod was used for the matrix as there was found to be a small number of super laves in the matrix measuring ~1 μm not able to be distinguishable due to the limited q range. Due to their smaller size, the nucleating and β phase precipitates are present in the high q range and were modelled using an ellipsoid and spherical function respectively. The chemistries of the matrix, laves and β phase were known from APT, and, further calculations determined the density of each phase as 8.1, 11, and 6.1 g/cm^3 respectively. The Scatter Length Density (SLD) was then calculated from these values [22], for example, the SLD was 7.237, 6.798 and 5.464 x 10^{-6} A^{-2} for the pre-existing laves, nucleating laves and β phase respectively austenitized at 825°C and aged 7.5 hrs at 540°C. Having both unaged and aged (7.5 hrs) chemistries from APT for austenitization at 825 and

960°C, the chemistries were not refined when fitting the SANS model. Table 4 lists the refined parameters of interest for the model described here:

Table 4. Refined parameters of interest of SANS model

Ellipsoid 1: Pre-existing Laves	**Ellipsoid 2: Nucleating Laves**	**Sphere: β Phase**
R_a	R_a	R
R_b	R_b	Scale S
Scale E_1	Scale E_2	

With four phases present there is a concern over the number of refined parameters. Fig. 4 shows that each extreme of the SANS spectra is dominated by only two functions with the low *q* range dominated by the matrix and pre-existing laves, and, the high *q* range being predominantly nucleating laves and β phase. As the unaged condition is known to have only the matrix and pre-existing laves, the chosen functions were fitted. This fit was them rolled over to the 1 hr aged condition which then introduces the nucleating precipitates. The ability to progressively fit coupled with size variation of the precipitates meant that good stable fits were achieved that were corroborated by various APT, SEM, and TEM images taken at 7.5 hrs aging.

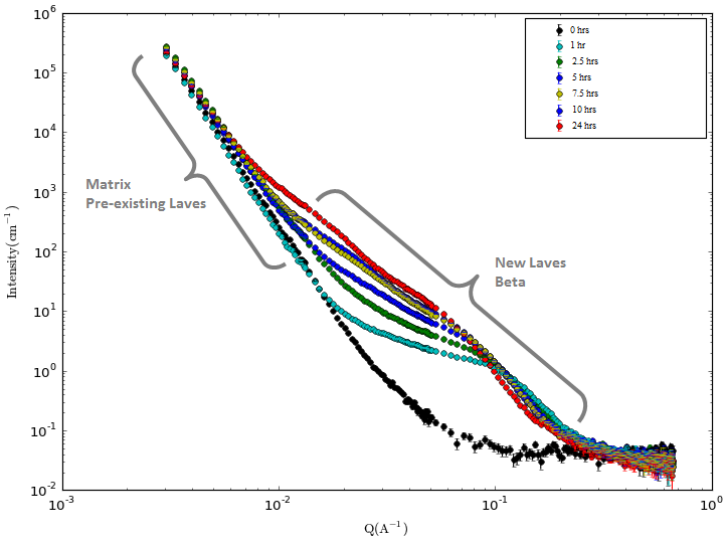

Figure 4. Aging time progression of SANS spectra for 870°C austenitization

Fig. 5 shows a typical fit for the 'Guinier Porod + Ellipsoid + Ellipsoid + Sphere' model to the SANS. The drop in intensity at high *q* is considered to be linked with changes in the super laves which measure beyond the *q* range examined here. The model reproduces the overall intensity as well as the undulating features seen in the high *q* range. Polydispersity of 0.2 was implemented for the β particles and 0.15 for both populations of laves. These values were determined from APT and not refined in order to limit variables. A common approach is to fix the aspect ratio of the precipitates within the SANS model, this was unnecessary as reliable and stable fits were obtained and the shape of the precipitate may have implications on mechanical properties which is to be explored at a later date.

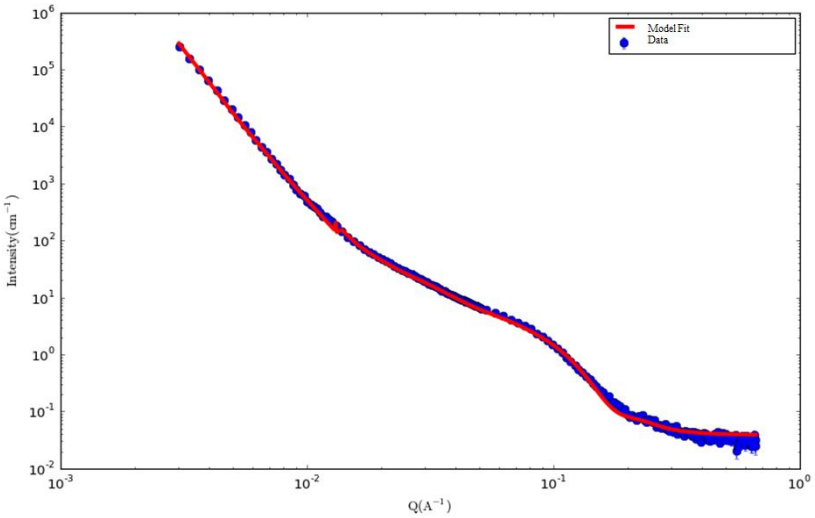

Figure 5. Example of model fit to SANS data using SASview. Blue points denote data with error, and, red line denotes fit.

4. Results and Analysis

In the following analysis pre-existing laves located at grain boundaries, present in the unaged condition are termed Laves 1. Laves 2 are the laves that nucleate and grow under thermal aging.

3.1 Austenitization

Fig. 6 shows the size and volume fraction of Laves 1 precipitates during aging at 540 °C for the three austenitization temperatures. As expected from Fig. 1, in the unaged condition, lower austenitization temperatures produce more Laves 1 with the highest austenitization temperature having almost none. As the material is aged, Laves 1 grows in both volume fraction and size with precipitate numbers throughout reasonably constant. Lower austenitization temperatures result in more Laves 1 at long aging times reversing the initial Laves 1 trend in the unaged condition. At lower austenitization temperatures faster growth rates potentially were observed potentially due to fewer pre-existing laves in the unaged

condition, this is consistent with phase forming elements being present and undepleted within the matrix.

a)

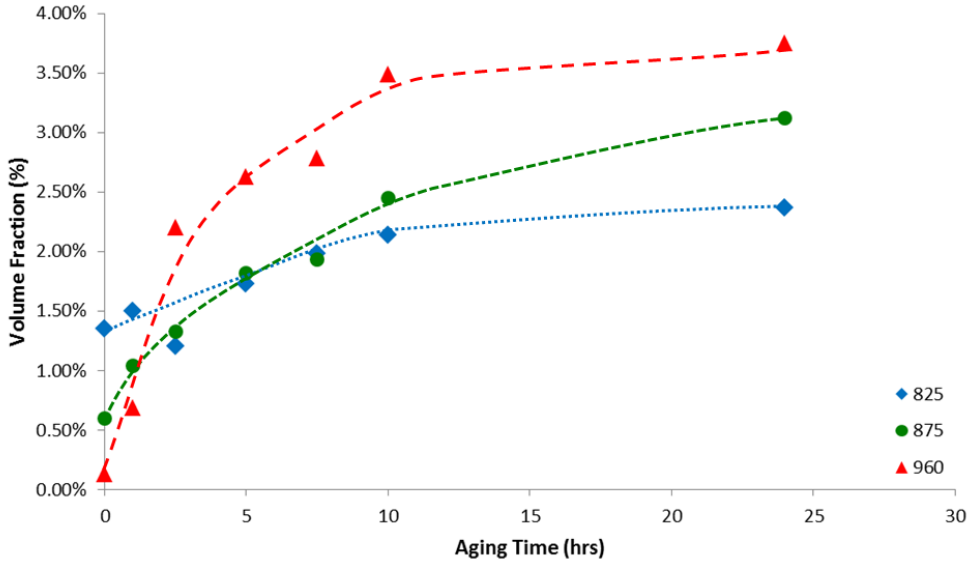

b)

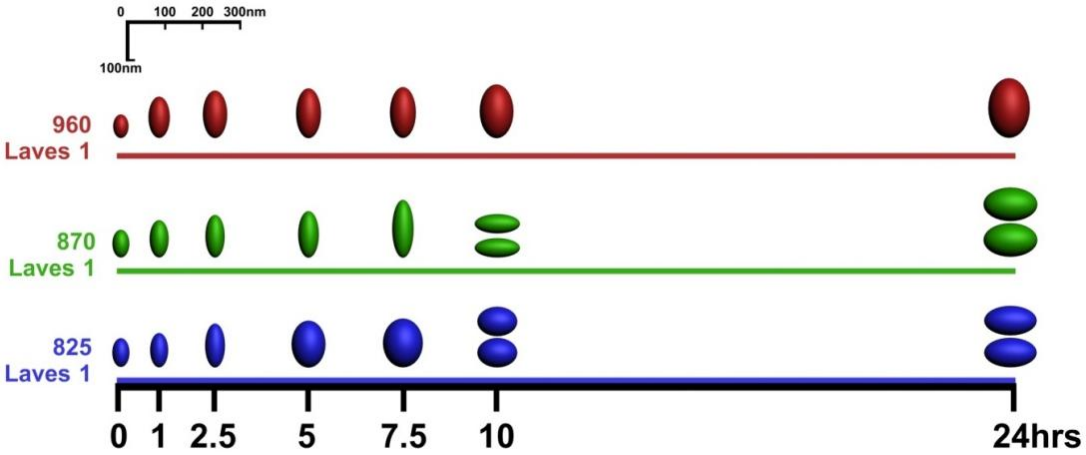

Figure 6. Austenitization temperature dependence of Laves 1; a) volume fraction, and b) size with aging time

For the 825 and 870 °C austenitization aged for 10 hrs, a significant decrease in precipitate size with an increasing volume fraction is observed. According to the SANS model, the

decrease in size coincides with an approximate halving of the long axis of the Laves 1 between 7.5 and 10 hrs for both conditions and with the short axis continuing to grow. With q_{min}~0.003 A^{-1}, the spectra measured covers precipitates up to approximately 210 nm. If the precipitate continued to grow then its length would be ~180 nm at 10 hrs and detectable. This change in length for the 825 °C austenitization can be seen in the spectra shown in Fig. 7a at with an increase in intensity at Q < 10^{-2} $Å^{-1}$, which is not seen in Fig. 7b for austenitization at 960 °C.

a)

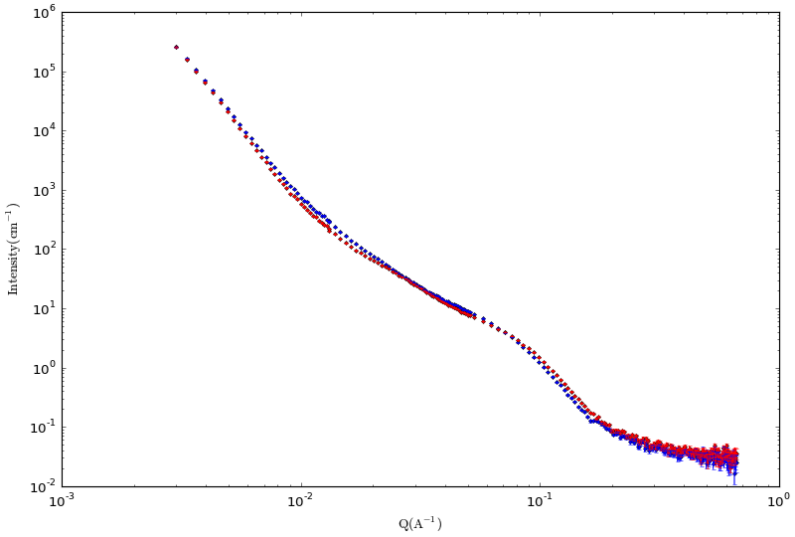

b)

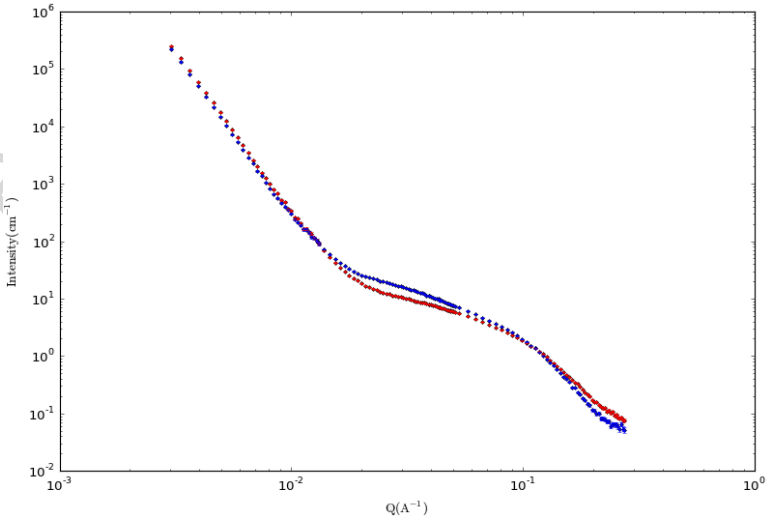

Figure 7. SANS spectra for a) austenitization at 960 °C aged at 540 °C for 7.5hrs (red) and 10 hrs (blue), and, b) austenitization at 825 °C aged at 540 °C for 7.5hrs (red) and 10 hrs (blue)

Indeed, when we look at the precipitates via back scattered SEM in Fig 8., we observe this decrease in precipitate size at 10 hrs compared to 7.5 hrs for austenitization at 825°C (Fig. 8a & 8b) but not at 960°C (Fig. 9c & 8d). From the SANS, it suggests that the Laves 1 precipitate may undergo precipitate splitting.

a)

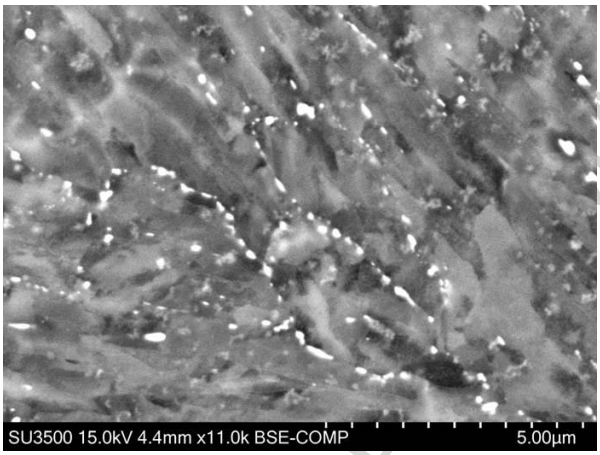

b)

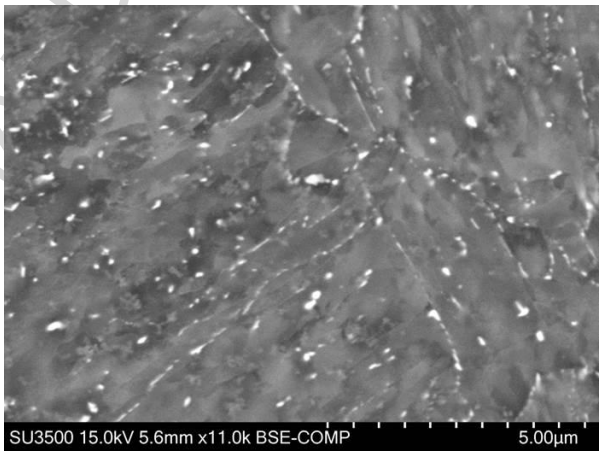

c)

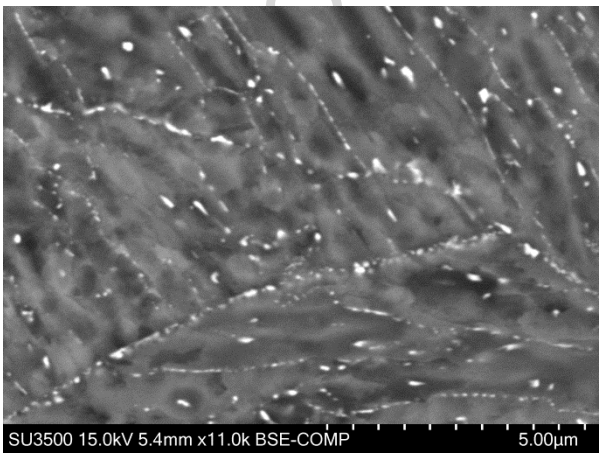

d)

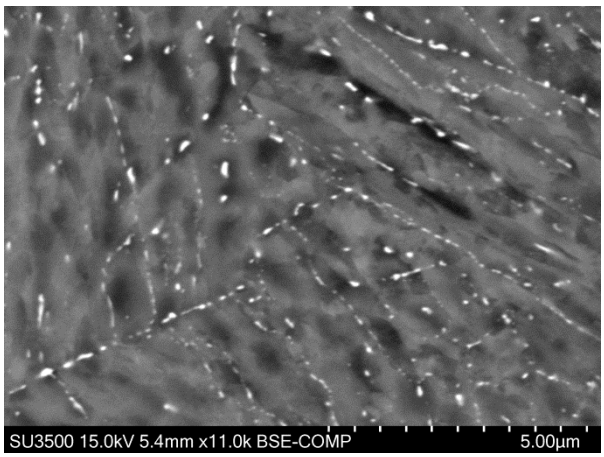

Figure 8. Backscattered electron microscopy of F1E austenitized at 825°C and aged at 540°C for a) 7.5 hrs, and b) 10 hrs, and austenitized at 960°C and aged at 540°C for c) 7.5 hrs, and d) 10 hrs

During aging a second population of laves nucleates and grows, these designated here as Laves 2. From Fig. 9a we see a plateau or retardation in growth of Laves 2 at 5, 5 and 2.5 hrs for austenitization at 825, 875 and 960°C respectively. These points precede the Laves 1 precipitate splitting for austenitization at 825 and 875°C, with the case of 960°C discussed in more detail later. From this information Laves 1 development is seen to have an impact on element availability and thus the growth of Laves 2.

a)

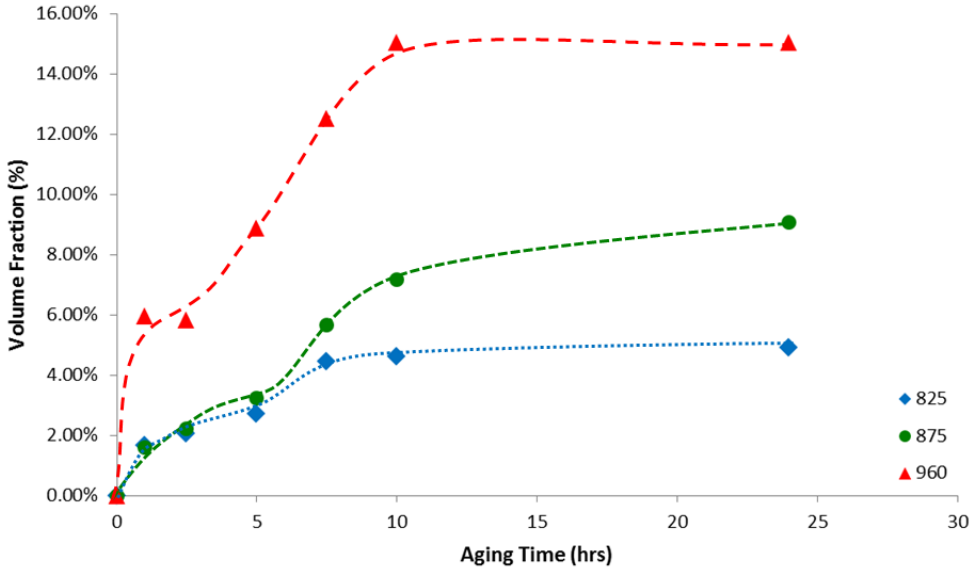

b)

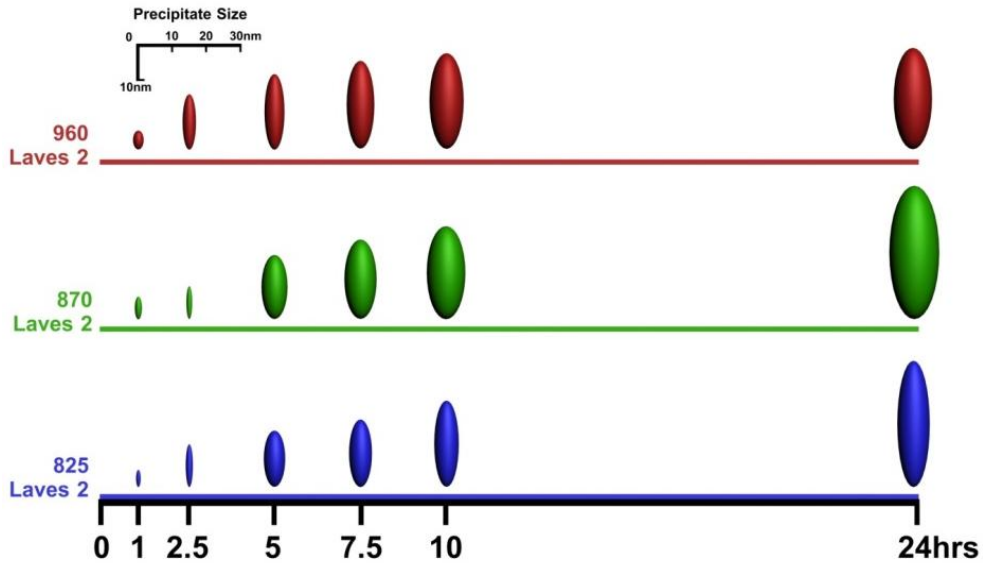

Figure 9. Austenitization temperature: Laves 2 a) volume fraction, and b) size with aging time

For Laves 2, a marked difference is observed between volume fraction depending on austenitization temperature with the higher austenitization temperature of 960°C producing

substantially more Laves 2 when aged. This trend is also seen for Laves 1 but less exaggerated.

The last precipitate of interest is the NiAl rich β-phase. From Fig. 10, a higher austenitization temperature produces slightly less β with all conditions producing similar sized precipitates. After aging for 5 hrs, the population and size of the β precipitates has plateaued.

a)

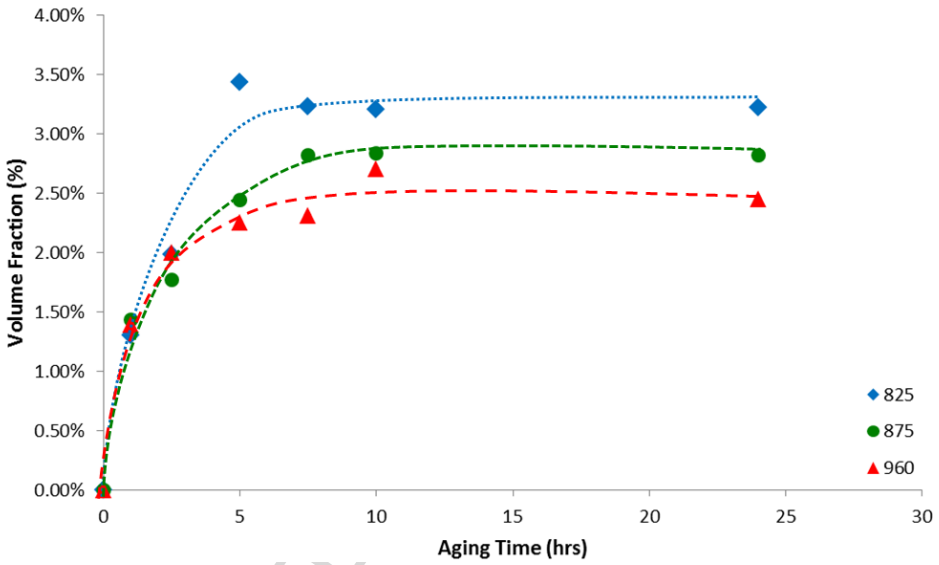

b)

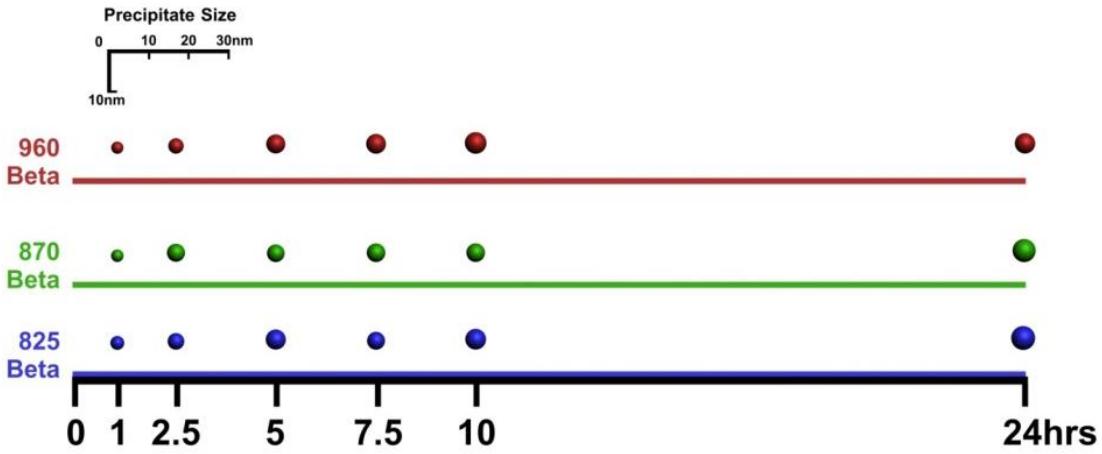

Figure 10. Austenitization temperature: β-phase a) volume fraction, and b) size with aging time

3.3 Aging

Choosing one austenitization condition and changing the aging temperature allows its impact on precipitate development to be assessed. Using F1E austenitized at 960°C the material was aged at three different temperatures: 520, 540 and 560°C. The same aging times of 1, 2.5, 5, 7.5, 10 and 24 hrs were observed with the exception for 520°C 24 hrs.

a)

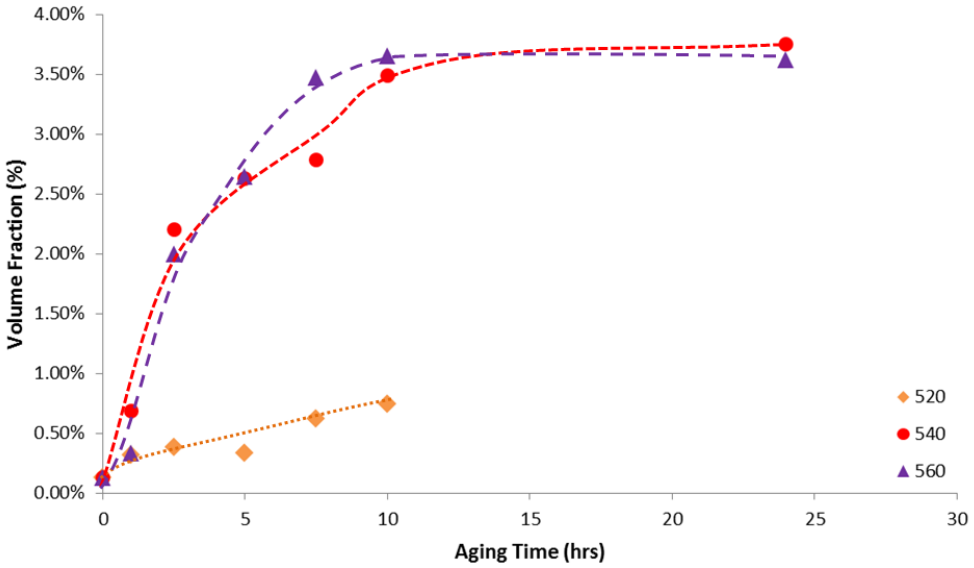

b)

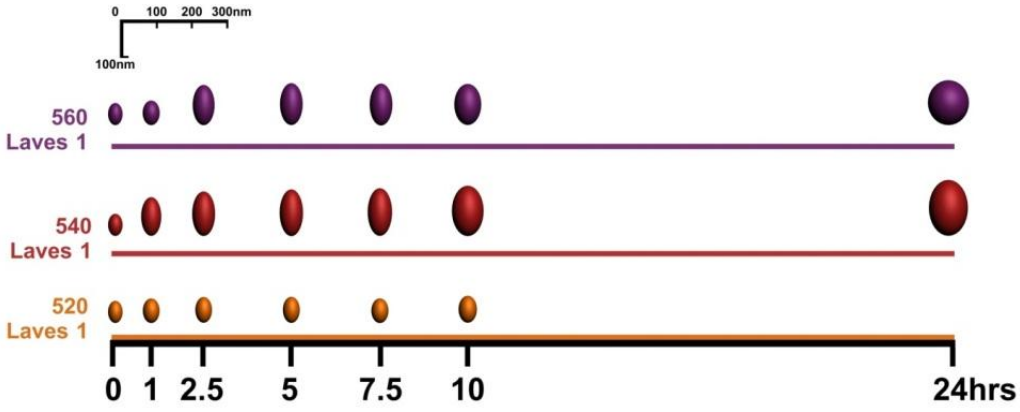

Figure 11. Aging temperature: Laves 1 a) volume fraction, and b) size with aging time

From Fig. 11, aging at 540 and 560°C produce similar growth rates and amounts of Laves 1 with the higher temperature producing slightly rounder laves. Aging at 520°C produces very little growth of the pre-existing laves, clearly observable in the SANS spectra.

For Laves 2, Fig. 12 shows aging at 520°C produces a very small amount of Laves 2 meaning both populations of laves experience retarded growth at 520°C. For the 540 and 560°C similar laves volume fractions and growth rates are observed to one another, with the higher aging temperature producing narrower Laves 2.

a)

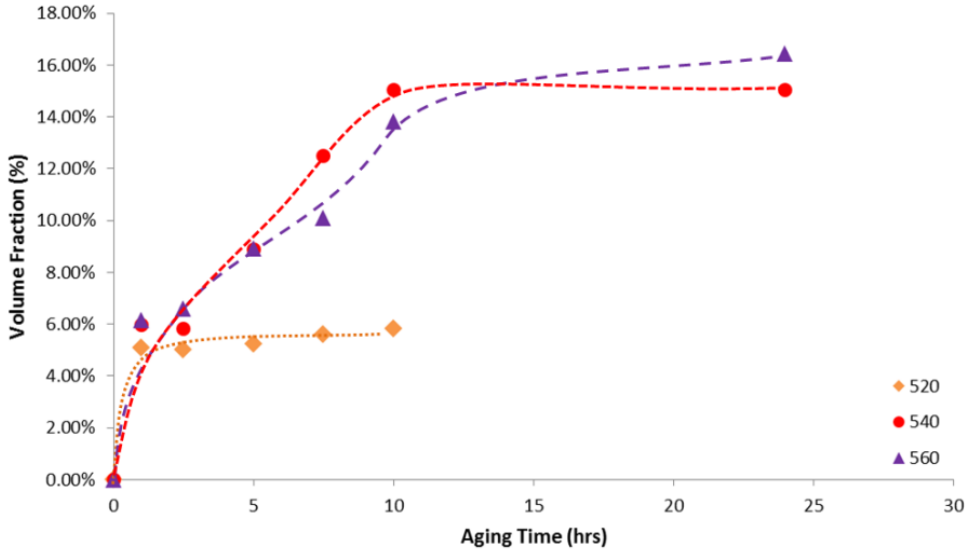

b)

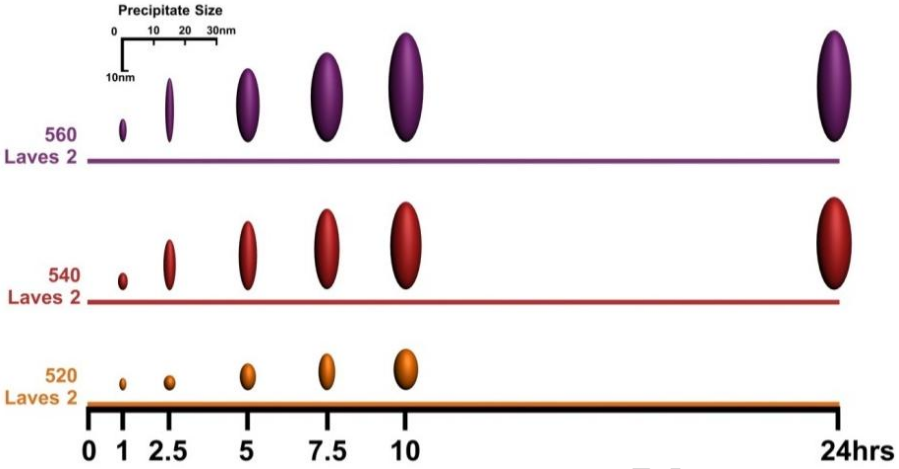

Figure 12. Aging temperature: Laves 2 a) volume Fraction, and b) size with aging time

Unlike the austenitization temperature, aging temperature affects both β-phase volume fraction and size. In Fig. 13, higher aging temperatures are observed to produce progressively larger but fewer β precipitates, whilst colder condition produce a greater volume of particles of a smaller size. The growth rate of β shows a lower aging temperature causes plateauing in size and volume fraction later than under hotter conditions. The lower aging temperature producing a greater volume fraction of β may be due to less laves competing for elements.

a)

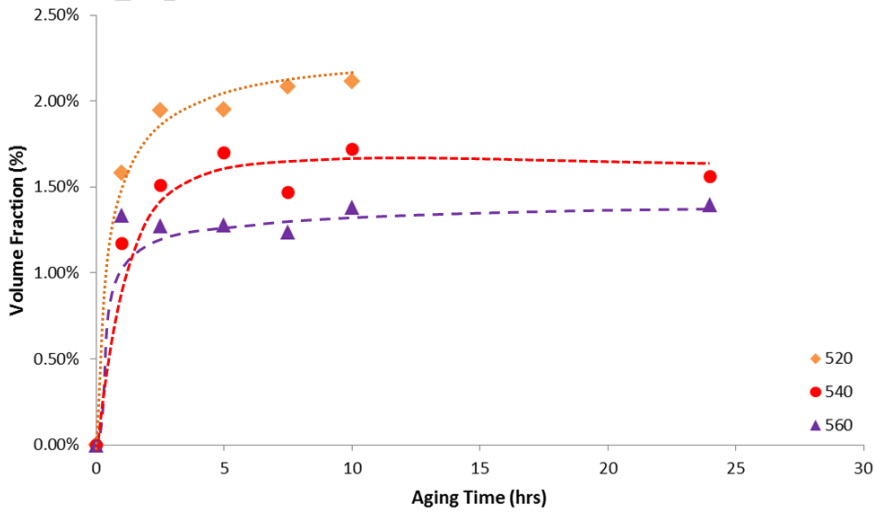

b)

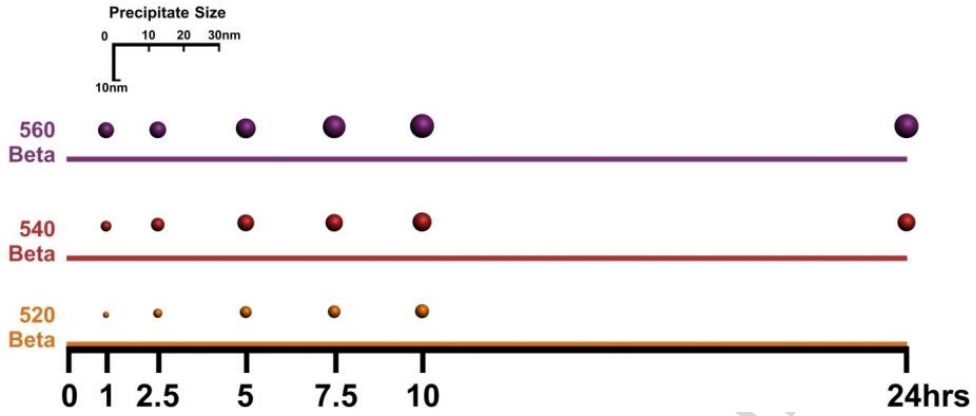

Figure 13. Aging temperature: β-phase a) volume fraction, and b) size with aging time

5. Discussion

This experiment has produced two unexpected results. The lesser of the two is the lack of laves growth when aged at 520°C. SANS spectra for samples austenized at 960°C and aged for 7.5 hours at 520 and 540°C is shown in Fig. 14. There is a notable lack of intensity around q=1x10^{-2}Å^{-1} which is observed across all spectra aged at 520°C.

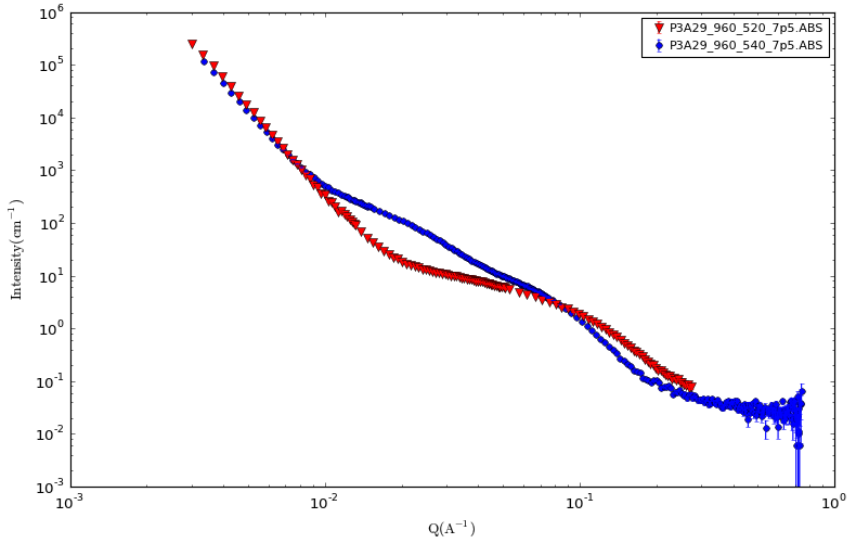

Figure 14. Comparison of SANS spectra austenitized at 960°C and aged for 7.5 hours at 540°C (blue dots), and 520°C (red triangles)

Given this lack of precipitate growth was not predicted by thermal calculations as shown in Fig. 1, further investigations needs to be conducted into whether this retardation is due to austenitization and aging conditions combined, or whether aging at 520°C has insufficient thermal energy to drive growth in all conditions.

The most unexpected outcome of the SANS analysis was the observation of 'precipitate splitting' for the 825 and 870°C austenitized condition aged at 540°C for 7.5-10 hours (see Fig. 6). Although not rigorously observed for steels, precipitate splitting is potentially present in the work of Lietner *et al.* [23]. This work observed the growth of a precipitate that, when thermally aged at 525°C for 3 hrs, decomposed into η-phase and β-phase precipitates. Looking to nickel super alloys, precipitate splitting is more common where γ' has been observed to decompose from a cuboid to a doublet [24]. Investigations by Khachaturyan suggest this occurs when a precipitate exceeds a critical size and the elastic strain energy dominates over the precipitate/matrix interfacial energy [25-26]. From Fig. 6b there is a substantial difference in the aspect ratio of Laves 1 related to the austenitization condition that is not yet fully understood, and as such the normalised values were considered. Normalising the long axis measurement of the fitted ellipse by its value at 0 hrs aging, Fig. 15 graphs this value versus aging time for the three austenitization conditions. Once the Laves 1 grows to double its original length, from a SANS perspective it appears to split for the 825 and 870°C austenitization, no precipitate splitting was observed for austenitization at 960°C potentially due to the minimal amount of Laves 1 present or splitting occurring so early it is undetected.

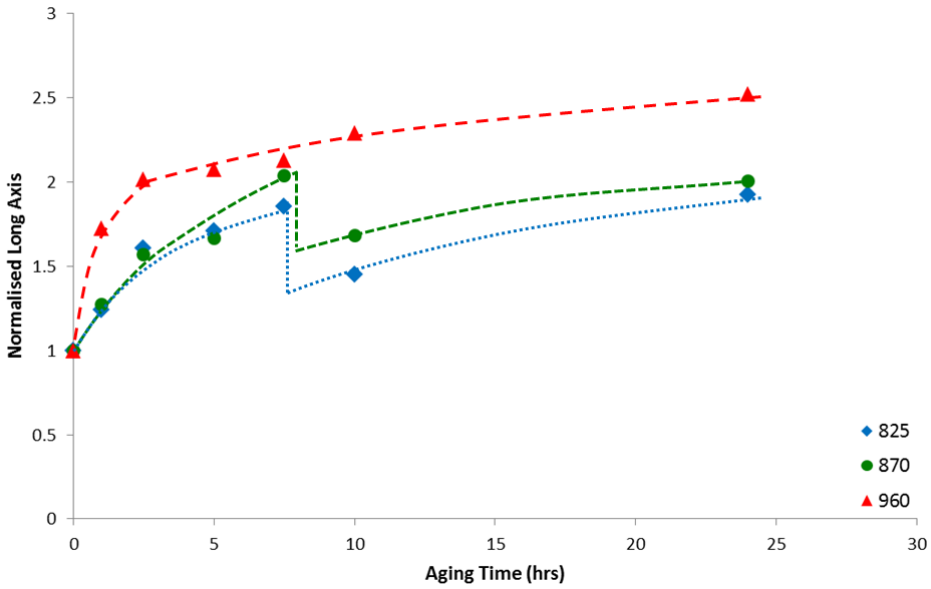

Figure 15. Dimensions of Laves 1: normalised long axis vs. aging time

A different suggestion for precipitate splitting in nickel is that there may be a fluctuation from chemical equilibrium at the interface between the precipitate and matrix affecting diffusion [27]. In Fig. 16 using ATP on a sample austenitized at 825°C and aged for 5 hrs, a build-up of chromium on the surface of the laves is observed, highlighted in purple. Chromium was not observed on the surface of the unaged laves suggesting aging may cause a significant change in the chemistry surrounding the laves phase.

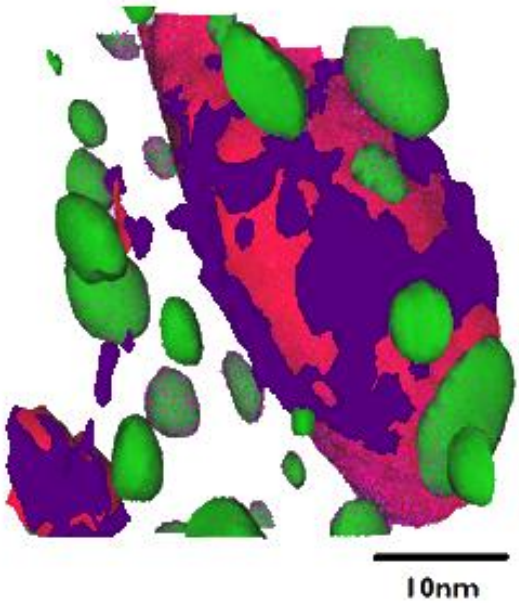

Figure 16. Chromium build-up due to aging on laves. Austenitized 825 °C and aged 5 hrs; Red=laves, green=β-phase, and purple=chromium.

From using SANS on a range of heat treatments, results suggest the occurrence of precipitate splitting. The general cause of precipitate splitting is either dimensional constraint or change in chemistry which is present in these conditions. From SEM-BSE images we see a significant change in the precipitate as well. Although these observations support the hypothesis of precipitate splitting as suggested by SANS, further work needs to be conducted in order to confirm this phenomenon.

6. Conclusions

Due to the presence of four different phases, a defined shape model was chosen to eliminate the freedom and flexibility of a statistical model. Using a defined shape model, it was possible to characterise the evolution of precipitates in the novel maraging steel F1E for a number of austenitization and aging temperatures, as well as, times. The lower austenitization temperature resulted in more laves being present before aging, and, once aged less growth in pre-existing and nucleating laves was observed. Opposite to this trend, a small increase in the amount of β-phase was observed for lower austenitization temperatures. When aging, the only marked difference came when aged at 520°C when laves growth was significantly retarded. Otherwise, the only difference between aging temperatures lies with the β-phase with the lower aging temperature producing more β.

For the austenitization condition of 825 and 870° C a change in microstructure at 7.5 hrs was observed. From the SANS, laves present from austenitization appear to split, with a halving of the long axis and no reduction in volume fraction. SEM conducted also confirms a change

in microstructure but does not definitely confirm precipitate splitting. The possibility of precipitate splitting in a steel is novel, but requires further investigation as both the geometric and chemical conditions for initiating splitting are present. Observations from APT show a build-up of chromium on the surface of these laves which in this research has not been fully considered. Further work identifying what microstructural and chemical changes occurring needs to be conducted to fully characterise these phenomena.

Presented in this work is a large scale study of austenitization and aging conditions for a novel maraging steel. Using a number of techniques in conjunction with SANS the growth and evolution of precipitates was observed which are linked to the mechanical properties of this aerospace material. By conducting this study we have observed unexpected precipitate behaviour but also gained wider knowledge of the material which when linked to mechanical data provides a means to tailor heat treatments and effectively create bespoke components adapted specifically to their purpose.

Acknowledgements.

This work has been funded by the Rolls-Royce plc. Strategic Partnership in Structural metallic systems for advanced gas turbine applications, EPSRC (EP/H500383/1). We acknowledge the support of the Australian Centre for Neutron Scattering, Australian Nuclear Science and Technology Organisation, in providing neutron research facilities and support.

References

[1] D.E.R. Petty, Martensite: Fundamentals and Technology, Longman, London, 1970.

[2] M.P. Boyce, Gas Turbine Engineering Handbook, 3rd Edition, Gulf Professional Publishing, Oxford, 2006

[3] S. McAdams, PhD Thesis: The mechanical characterisation of a high strength, creep resistant steep for aerospace applications, Swansea University, April 2014

[4] H.J. Rack, D. Kalish, Improvement in fatigue resistance of 18Ni(350) maraging steel through thermo-mechanical treatments, Metall. Trans. A 5(1974) 685–694

[5] W. Sha, Y. He, K. Yang, D.J. Cleland, Microstructure and mechanical properties of a 2000 MPa Co-free maraging steel after ageing at 753K, Metall. Trans. A 35 (2004) 2747–2755

[6] H.K.D.H. Bhadesia, R. Honeycombe, Steels: Microstructure and Properties, 3rd Edition, Amsterdam, Butterworth-Heinemann (Elsevier), (2006)

[7] Rolls-Royce plc., PO Box 31, Derby DE24 8BJ, UK.

[8] ATI Specialty Metals: Allvac, Monroe NC 281110, USA, https://www.atimetals.com/businesses/ATISpecialtyMaterials/Pages/default.aspx,

[9] R.H. Davies, A.T. Dinsdale, J.A. Gisby, J.A.J. Robinson, S.M. Martin, MDATA-Thermodynamics and Phase Equilibrium Software from the National Physical Laboratory, CALPHAD 26 (2002) 229-271

[10] B. Gault, Atom Probe Microscopy, New York, Springer, 2012

[11] E.P. Gilbert, J.C. Schulz, T.J Noakes, Quokka'–the small-angle neutron scattering instrument at OPAL, Physica B 385–386 (2006) 1180–1182

[12] S.R. Kline, Reduction and analysis of SANS and USANS data using IGOR Pro, J. Appl. Crystal. 39 (2006) 895-900

[13] Irena for Igor, Argonne National Laboratory, Used 28/11/2014, http://usaxs.xray.aps.anl.gov/staff/ilavsky/irena.html

[14] Quokka User Manual, Version: October 2015, http://www.ansto.gov.au/cs/groups/corporate/documents/document/mdaw/mdm4/~edisp/acs079538.pdf

[15] SaSview Version 3.0.0, Installed 15/01/2015, http://www.sasview.org/

[16] A. Guinier, G. Fournet, Small-Angle Scattering of X-Rays, John Wiley and Sons, New York, 1955

[17] O. Glatter, O. Kratky, Small-Angle X-Ray Scattering, Academic Press, London, 1982

[18] A. Guinier, G. Fournet, Small-Angle Scattering of X-Rays, John Wiley and Sons, New York, 1955

[19] SANS Model Function Documentation Version 4, February 2008, Accessed 20/01/2015, http://www.ncnr.nist.gov/programs/sans/data/Download/SANS_Model_Docs_v4.00.pdf

[20] L.A. Feigin, D.I. Svergun, Structure Analysis by Small-Angle X-Ray and Neutron Scattering, Plenum Press, New York, 1987

[21] S. Kline, A Munter, Ellipsod Model, Accessed 04/09/2015, http://www.ncnr.nist.gov/resources/sansmodels/Ellipsoid.html

[22] Neutron Activation and Scattering Calculator, NIST Centre for Neutron Research, Accessed 30/03/2015, http://www.ncnr.nist.gov/resources/activation/

[23] H. Leitner, M. Schober, R. Schnitzer, Splitting phenomenon in the precipitation evolution in an Fe–Ni–Al–Ti–Cr stainless steel, Acta Mat. 58 (2010) 4 1261-1269

[24] M. Doi, T. Miyazaki, The effect of elastic interaction energy on the shape of γ'-precipitate in Ni-based alloys, Superalloys (1984) 543-552

[25] A.G. Khachaturyan 1983 Theory of Structural Transformation in Solids Wiley, New York, 1983

[26] G. Khachaturyan, S.V. Semenovskaya, J.W. Morris, Theoretical analysis of strain-induced shape changes in cubic precipitates during coarsening, Acta Metall. 36 (1988) 1563-1567.

[27] Y. Yamabe-Mitarai, H. Harada, Formation of a 'splitting pattern' associated with L1 2 precipitates in Ir-Nb alloys, Phil. Mag. Lett. 82 (2002) 109–118

Highlights

- Large scale study of precipitate growth (laves and β phase) in a novel maraging steel integrating knowledge from APT, TEM, SEM, and STEM into SANS modelling and analysis
- Effect of 3 different austenitization temperatures studied
- Effect of 3 different aging temperatures studied
- Effect of aging time studied at 0, 1, 2.5, 5, 7.5, 10 and 24 hrs
- Laves phase precipitate undergoes previously unknown microstructural change during aging